Proceedings of the 7th WSEAS International Conference on Mathematics & Computers in Biology & Chemistry, Cavtat, Croatia, June 13-15, 2006 (pp13-18)

Identification of motor unit discharge patterns in time-frequency plane

ALES HOLOBAR, DAMJAN ZAZULA
Faculty of Electrical Engineering and Computer Science
University of Maribor
Smetanova ulica 17, 2000 Maribor
SLOVENIA
ales.holobar@uni-mb.si, zazula@uni-mb.si, http://*storm.uni-mb.si/*

Abstract: - This paper presents a novel approach to decomposition of multichannel surface electromyograms recorded during low-level isometric muscle contractions. The approach is based on special time-frequency matrices of measured signals, enables separation of contributions of different motor units in time-frequency plane and is not sensitive to the superimpositions of motor unit action potentials. The results on both synthetic and real surface electromyograms prove the proposed approach is robust to noise and has potential clinical applications for the non-invasive analysis of single motor unit properties.

Key-Words: - Surface electromyogram, Motor unit discharge pattern, Blind Source Separation, Time-Frequency domain

1 Introduction

Pathological changes in human neuromuscular system are associated with rising health care use, disability, and financial costs. Only in EU approx. 170 million working days is lost annually due to the health problems related to musculoskeletal disorders. Tools for objective and periodical assessment of motor function in humans are needed but are currently lacking.

Human skeletal muscles comprise up to several hundreds of motor units (MU), i.e. small functional groups of muscle fibers. All fibers belonging to the same MU are innervated by the same motor neuron which transmits the control commands from the central nervous system in a form of innervation pulse trains. Each pulse in the innervation train triggers the so called motor unit action potential (MUAP), i.e. a measurable electrical potential, which travels from the innervation zone towards tendon regions causing the muscle fibers to contract. Usually, sufficiently large number of MUs contracts asynchronously to produce a random interference pattern, called electromyogram (EMG). Speaking about quantitative indicators of neuromuscular system condition, there is no real alternative to EMG [10].

Practically all clinical EMG investigations are based on the needle (inter-muscular) electrodes, whose invasive character prevents the long-term monitoring of the electromuscular parameters. More advanced EMG recording techniques, which detect the EMG signals on the skin surface above the investigated muscle, offer numerous advantages. Firstly, there is no risk to tissue damage what allows for unlimited repetition of tests in exactly the same place. Secondly, surface EMG (SEMG) electrodes eliminate the need for miniaturization and sterilizations and are, hence, inexpensive when compared to the needle electrodes. Thirdly, the SEMG signal detected on the skin surface includes information from a greater proportion of the muscle under investigation and is therefore more representative than conventional but very selective needle EMG.

Despite its obvious potential, surface EMG is still rarely used in clinical settings. The main reason lies in a high complexity of SEMG signals and poor morphological information about the individual MUs. In the case of needle electrodes we can selectively observe the action potentials of only a few active MUs, or even of a single muscle fiber. In the SEMG case, on the other hand, we deal with several tens of concurrently active MUs. Moreover, the detected MUAPs vary in amplitude, duration and frequency and are further affected by the volume conductor separating MUs from detection system. Many attempts to enhance the information content of SEMG signals were made in the past, but quantitative analysis of single MUs remains very delicate process, even at low muscle contractions [10].

This paper presents a novel approach to identification of MU discharge patterns. Described algorithm operates in time-frequency (TF) plane and is based on very efficient blind-source separation

(BSS) technique. The paper is organized as follows. Section 2 describes the assumed SEMG data model. The decomposition approach is presented in Section 3, with the results form the experimental data reported in Section 4. We conclude the paper with the discussion in Section 5.

2 Assumed SEMG data model

SEMG recordings can be modelled as a multi-channel linear, time-invariant system, as long as they have been taken in stable, controllable, and stationary measurement session. This implies an isometric muscle contraction and avoiding of the appearance of fatigue-induced changes. Dealing with sampled multi-channel EMG recordings, the discrete, shift-invariant multiple-input-multiple-output (MIMO) modelling is most feasible. Each source (channel input) in such MIMO system is considered a MU innervation pulse train triggering the muscle fibers, while the system responses (channels) correspond to the MUAPs as captured by a spatial filter (pick-up electrodes):

$$x_i(n) = \sum_{j=1}^{N} \sum_{l=0}^{L-1} h_{ij}(l) s_j(n-l), \quad \text{i=1,...,}M \tag{1}$$

where, in vector notation, $\mathbf{x}(n) = [x_1(n), ..., x_M(n)]^T$ stands for vector of M surface measurements, $h_{ij}(l)$ denotes the *(i,j)*-th unit system response, i.e. the MUAP of the *j*-th MU as detected in the *i*-th measurements, and $\mathbf{s}(n) = [s_1(n), ..., s_N(n)]^T$ is the vector of N innervation pulse sources:

$$s_j(n) = \sum_{r=-\infty}^{\infty} \delta\left[n - T_j(r)\right], \quad \text{j=1,...,}N \tag{2}$$

with $T_j(r)$ denoting the time instant in which the *r*-th innervation pulse of *j*-th MU appeared.

Convolutive relationship described in (1) can always be expressed in matrix form:

$$\mathbf{x}(n) = \mathbf{H}\bar{\mathbf{s}}(n) \tag{3}$$

where $\mathbf{H}$ stands for the so called mixing matrix of size $M \times NL$ which contains the unit sample responses $h_{ij}(l)$:

$$\mathbf{H} = \begin{bmatrix} \mathbf{h}_{11} & \cdots & \mathbf{h}_{1N} \\ \vdots & \ddots & \vdots \\ \mathbf{h}_{M1} & \cdots & \mathbf{h}_{MN} \end{bmatrix} \tag{4}$$

with

$$\mathbf{h}_{ij} = \left[h_{ij}(0),\ h_{ij}(1),\ h_{ij}(2),\ \ldots, h_{ij}(L-1)\right] \tag{5}$$

denoting the $1 \times L$ vector of *(i,j)*-th systems response. The extended vector of sources $\bar{\mathbf{s}}(n)$ takes the following form:

$$\bar{\mathbf{s}}(n) = [s_1(n), ..., s_1(n-L+1), ..., s_N(n), ..., s_N(n-L+1)]^T \tag{6}$$

Vector of measurements $\mathbf{x}(n)$ can additionally be extended by *K-1* delayed repetitions of each measurement:

$$\bar{\mathbf{x}}(n) = [x_1(n), x_1(n-1), ..., x_1(n-K+1), ..., x_M(n-K+1)]^T \tag{7}$$

When the influence of noise is considered we get:

$$\bar{\mathbf{y}}(n) = \bar{\mathbf{x}}(n) + \bar{\boldsymbol{\omega}}(n) \tag{8}$$

where $\bar{\boldsymbol{\omega}}(n)$ denotes the extended version of the noise vector $\boldsymbol{\omega}(n) = [\omega_1(n), ..., \omega_M(n)]^T$.

3 Surface EMG Decomposition

Recently, very efficient and robust approach to separation of instantaneous mixtures of nonstationary sources was introduced by A. Belouchrani and M. Amin [2]. Their method exploits the differences in energy locations of sources in TF domain and is based on the joint diagonalization [5,6] of so called spatial time-frequency distribution (STFD) matrices:

$$\mathbf{D}_{\bar{\mathbf{x}}\bar{\mathbf{x}}}(n,f) = \sum_{l=-\infty}^{\infty} \sum_{m=-\infty}^{\infty} \boldsymbol{\Theta}(m,l) \bar{\mathbf{x}}(n+m+l) \bar{\mathbf{x}}^H(n+m-l) e^{-4\pi \cdot f \cdot l} \tag{9}$$

which are, for all possible pairs of measurements constructed from the TF distributions of Cohen class [7]:

$$\mathbf{D}_{x_i x_j}(n,f) = \sum_{l=-\infty}^{\infty} \sum_{m=-\infty}^{\infty} \boldsymbol{\varphi}(m,l) x_i(n+m+l) x_j^*(n+m-l) e^{-4\pi f l} \tag{10}$$

where $\boldsymbol{\Theta}(m,l)$ and $\boldsymbol{\varphi}(m,l)$ stand for the kernels that characterize the time-frequency distribution, respectively.

Neglecting the noise and considering linearity of the assumed MIMO system we can write:

$$\mathbf{D}_{\bar{\mathbf{x}}\bar{\mathbf{x}}}(n,f) = \mathbf{H}\mathbf{D}_{\bar{\mathbf{s}}\bar{\mathbf{s}}}(n,f)\mathbf{H}^T \tag{11}$$

where, for every fixed index pair (n,f), $\mathbf{D}_{\bar{\mathbf{s}}\bar{\mathbf{s}}}(n,f)$ denotes the STFD matrix of extended sources.

In the sequel, the off-diagonal elements of $\mathbf{D}_{\bar{\mathbf{s}}\bar{\mathbf{s}}}(n,f)$ matrices (cross-TF distributions) will be referred to as crossterms, while the diagonal elements of $\mathbf{D}_{\bar{\mathbf{s}}\bar{\mathbf{s}}}(n,f)$ will be called autoterms. As a result, matrices $\mathbf{D}_{\bar{\mathbf{s}}\bar{\mathbf{s}}}(n,f)$ will be diagonal if and only if all their crossterms will be equal to zero [9].

The blind separation approach introduced in [2] is based on assumption of more measurements than sources and comprises two steps. In the first step the extended vector of measurements $\bar{\mathbf{x}}(n)$ is spatially whitened by the matrix $\mathbf{W}$, which satisfies

$$\mathbf{W}\mathbf{R}_{\bar{\mathbf{x}}}\mathbf{W}^T = \mathbf{W}\mathbf{H}\mathbf{R}_{\bar{\mathbf{s}}}\mathbf{H}^T\mathbf{W}^T = \mathbf{I} \tag{12}$$

where $\mathbf{R}_{\bar{\mathbf{s}}}$ stands for sample correlation matrix of extended sources and $\mathbf{R}_{\bar{\mathbf{x}}}$ for the correlation matrix of extended measurements. Denoting the matrix

square root of $\mathbf{R}_{\bar{\mathbf{s}}}$ by $\mathbf{R}_{\bar{\mathbf{s}}}^{\frac{1}{2}}$ it is obvious from (12) that $\mathbf{U}=\mathbf{W}\mathbf{H}\mathbf{R}_{\bar{\mathbf{s}}}^{\frac{1}{2}}$ is a unitary matrix. The **W** matrix can be constructed as a matrix square root of the inverse of the $\mathbf{R}_{\bar{\mathbf{x}}}$ matrix [1, 2].

By multiplying the $\mathbf{D}_{\bar{\mathbf{x}}\bar{\mathbf{x}}}(n,f)$ matrices by **W** Eq. (11) yields the whitened STFD matrices [2, 3]:

$$\mathbf{D}_{\bar{\mathbf{z}}\bar{\mathbf{z}}}(n,f)=\mathbf{W}\mathbf{D}_{\bar{\mathbf{x}}\bar{\mathbf{x}}}(n,f)\mathbf{W}^{T}=\mathbf{U}\mathbf{R}_{\bar{\mathbf{s}}}^{-\frac{1}{2}}\mathbf{D}_{\bar{\mathbf{s}}\bar{\mathbf{s}}}(n,f)\mathbf{R}_{\bar{\mathbf{s}}}^{-\frac{1}{2}}\mathbf{U}^{T} \qquad (13)$$

Dealing with the SEMG signals, the upper limit of the MU discharge rate, random jittering of discharge rate and refractory period of muscle fibers guarantee the extended sources are orthogonal. As a result, $\mathbf{R}_{\bar{\mathbf{s}}}$ equals identity, and eliminates the unknown matrix $\mathbf{R}_{\bar{\mathbf{s}}}^{-\frac{1}{2}}$ in (13). Unknown unitary matrix **U** can now be estimated by joint diagonalization [4, 6]. However, to be able to do this we must first ensure the $\mathbf{D}_{\bar{\mathbf{s}}\bar{\mathbf{s}}}(n,f)$ matrices, which enter the reconstruction of matrix **U,** are also diagonal.

Generally speaking, the $\mathbf{D}_{\bar{\mathbf{s}}\bar{\mathbf{s}}}(n,f)$ matrices are, even in the case of SEMG signals, block diagonal. The reason is hidden in the kernel $\boldsymbol{\varphi}(m,l)$ of TF distributions, which is used to average the sources in time and, hence, spreads the information around individual MU innervation pulses. Excluding the kernel $\boldsymbol{\varphi}(m,l)$ from (10) we drive to so called Wigner-Ville TF distribution:

$$\mathbf{D}_{\bar{x}_i\bar{x}_j}(n,f)=\sum_{l=-\infty}^{\infty}\bar{x}_i(n+l)\bar{x}_j^{*}(n)e^{-4\pi\cdot f\cdot l} \qquad (14)$$

But Wigner-Ville spectra suffer from high sensitivity to the crossterms, which, again, make the source STFD matrices block diagonal. Namely, cross Wigner-Wille distribution of the *i*-th and *j*-th sources in an arbitrary time point n_k is a summation of all the pulses from the *i*-th and *j*-th sources, which satisfy the following relation:

$$n_k=\tfrac{1}{2}(n_{i,p}+n_{j,q}) \qquad (15)$$

where $p,q\in(-\infty,\infty)$ and $n_{i,p}$ ($n_{j,q}$) denotes the time moment in which the *p*-th (*q*-th) pulse of the *i*-th (*j*-th) source appeared. In other words, the cross TF distribution $\mathbf{D}_{\bar{s}_i\bar{s}_j}(n,f)$ differs from zero in every time moment which lies exactly in the middle between the arbitrary pulses of the *i*-th and *j*-th source.

We can reduce the number of pulses contributing to $\mathbf{D}_{\bar{s}_i\bar{s}_j}(n,f)$ by shrinking the calculation of the Wigner-Wille spectra in (14) to the finite interval [*-a,a*]:

$$\mathbf{D}_{\bar{x}_i\bar{x}_j}(n,f)=\sum_{l=-a}^{a}\bar{x}_i(n+l)\bar{x}_j^{*}(n)e^{-4\pi\cdot f\cdot l} \qquad (16)$$

where *a* denotes positive integer number. Setting the limit *a* to zero, all the crossterms are left out and the $\mathbf{D}_{\bar{\mathbf{s}}\bar{\mathbf{s}}}(n,f)$ matrices begin to show their diagonal structure. The TF distribution in (14) now yields:

$$\mathbf{D}_{\bar{x}_i\bar{x}_j}(n,f)=\bar{x}_i(n)\bar{x}_j^{*}(n) \qquad (17)$$

Having ensured the diagonality of the $\mathbf{D}_{\bar{\mathbf{s}}\bar{\mathbf{s}}}(n,f)$ matrices, we can use the joint diagonalization of several $\mathbf{D}_{\bar{\mathbf{s}}\bar{\mathbf{s}}}(n,f)$ matrices to reconstruct the missing unitary matrix **U**. Knowing the matrices **W** and **U**, the mixing matrix **H** can be estimated as

$$\mathbf{H}=\mathbf{W}^{\#}\mathbf{U} \qquad (18)$$

where $^{\#}$ denotes Moore-Penrose pseudoinverse. The sources can be reconstructed as:

$$\bar{\mathbf{s}}(n)=\mathbf{U}^{H}\mathbf{W}\bar{\mathbf{x}}(n)\,. \qquad (19)$$

3.1 Decomposition of close-to-orthogonal sources

In the previous section we supposed the sources are strictly orthogonal. This implies several restrictions that are hard to meet in reality. Processing the EMG signals, for example, the innervation pulse trains will be independent only at very low levels of muscle contractions. When the contraction level increases the innervation trains become more and more correlated (up to 10 %) and their pulses begin to overlap.

Let $G_{n_0}=\{j_{1,n_0},....,j_{p,n_0}\}$ denote a set of indices of sources which all trigger in a given time moment n_0. $\mathbf{D}_{\bar{\mathbf{s}}\bar{\mathbf{s}}}(n_0,f)$ matrix will be far from diagonal as it will have p^2 elements different from zero (all autoterms and all crossterms at the positions that are contained in G_{n_0}). Using the eigendecomposition $\mathbf{D}_{\bar{\mathbf{s}}\bar{\mathbf{s}}}(n_0,f)=\mathbf{U}_{\Lambda}\boldsymbol{\Lambda}\mathbf{U}_{\Lambda}^{T}$ we can write

$$\mathbf{D}_{\bar{\mathbf{z}}\bar{\mathbf{z}}}(n_0,f)=\mathbf{U}\mathbf{U}_{\Lambda}\boldsymbol{\Lambda}\mathbf{U}_{\Lambda}^{T}\mathbf{U}^{T} \qquad (20)$$

Hence, the diagonalization of $\mathbf{D}_{\bar{\mathbf{z}}\bar{\mathbf{z}}}(n_0,f)$ produces the wrong unitary matrix $\mathbf{U}\mathbf{U}_{\Lambda}$.

There is yet another condition that has to be met. To guarantee the uniqueness of the reconstructed unitary matrix **U,** the set of STFD matrices entering the joint diagonalization must contain the contributions of all extended sources [5, 9]. But, to guarantee their diagonality in the column-space of matrix **U**, each individual STFD matrix must contain the contribution of a single source only. This implies

that we must diagonalize at least $N(L+K-1)$ STFD matrices $\mathbf{D}_{\bar{\mathbf{z}}\bar{\mathbf{z}}}(n,f)$ (one for each source).

In other words, to guarantee the reconstruction of original mixing matrix we must be able not only to distinguish between the diagonal and nondiagonal $\mathbf{D}_{\bar{\mathbf{s}}\bar{\mathbf{s}}}(n,f)$ matrices, but also to distinguish between the matrices with contributions of different extended sources. With unitary matrix **U** unknown we can only rely on the information contained in the $\mathbf{D}_{\bar{\mathbf{z}}\bar{\mathbf{z}}}(n,f)$ matrices.

Let $\mathbf{D}^{i}_{\bar{\mathbf{s}}\bar{\mathbf{s}}}(n,f)$ denote the diagonal STFD matrix of sources with a single nonzero autoterm d_{ii} at the *i*-th diagonal position (i.e. with contribution from the *i*-th extended source). Bearing in mind that **U** is unitary we can derive the following relation:

$$\mathbf{D}^{i}_{\bar{\mathbf{z}}\bar{\mathbf{z}}}(n,f)\mathbf{D}^{j}_{\bar{\mathbf{z}}\bar{\mathbf{z}}}(n,f)=\mathbf{U}\mathbf{D}^{i}_{\bar{\mathbf{s}}\bar{\mathbf{s}}}(n,f)\mathbf{D}^{j}_{\bar{\mathbf{s}}\bar{\mathbf{s}}}(n,f)\mathbf{U}^{T}=0 \quad (21)$$

Now, denote by $\mathbf{D}^{ij}_{\bar{\mathbf{s}}\bar{\mathbf{s}}}(n,f)$ the STFD matrix of sources with contributions of both the *i*-th and *j*-th extended sources. $\mathbf{D}^{ij}_{\bar{\mathbf{s}}\bar{\mathbf{s}}}(n,f)$ will have four nonzero elements d_{ii}, d_{ij}, d_{ji} and d_{jj} at the positions (*i*,*i*), (*i*,*j*), (*j*,*i*) and (*j*,*j*), respectively. Short algebraic manipulation shows:

$$\left\langle \mathbf{D}^{ij}{}_{\bar{\mathbf{z}}\bar{\mathbf{z}}}(n,f),\mathbf{D}^{i}{}_{\bar{\mathbf{z}}\bar{\mathbf{z}}}(n,f)\right\rangle = d_{ii} \quad (22)$$

where scalar product $\langle . \rangle$ is defined as:

$$\left\langle \mathbf{M}_1,\mathbf{M}_2\right\rangle = \frac{trace(\mathbf{M}_1\mathbf{M}_2)}{trace(\mathbf{M}_2)} \quad (23)$$

and *trace(***M***)* denotes the sum of diagonal elements of matrix **M** (the matrix trace).

According to (21) and (23) the STFD matrices of whitened measurements with a contribution from a single source form the orthogonal basis of $N(L+K-1)$-dimensional space. The quest for $\mathbf{D}^{i}{}_{\bar{\mathbf{z}}\bar{\mathbf{z}}}(n,f)$ matrices with contributions from single, but different sources has now reduced to much easier problem of finding the orthogonal basis of the $N(L+K-1)$-dimensional space. This is a very important result as the criterion function (23) enables us to control the $\mathbf{D}_{\bar{\mathbf{z}}\bar{\mathbf{z}}}(n,f)$ matrices entering the joint diagonalization, and, consequently, guarantees the uniqueness of matrix **U**. We must still ensure the set of the $\mathbf{D}_{\bar{\mathbf{z}}\bar{\mathbf{z}}}(n,f)$ matrices entering the joint diagonalization contains the matrices with contributions from all the sources.

3.2 Influence of Noise

By minimizing the interval *[a,a]* on which the Wigner-Ville distribution is calculated we annulled the time averaging of measurements and, hence, reduced the robustness against noise [5]. The time averaging can be partially replaced by averaging of the $\mathbf{D}_{\bar{\mathbf{z}}\bar{\mathbf{z}}}(n,f)$ matrices with contributions from a single (not necessarily the same) source:

$$\frac{1}{T}\sum_{j=1}^{T}\left[\mathbf{D}^{i}_{\bar{\mathbf{z}}\bar{\mathbf{z}}}(n_j,f)\right]=\mathbf{U}\left[\frac{1}{T}\sum_{j=1}^{T}\mathbf{D}^{i}_{\bar{\mathbf{s}}\bar{\mathbf{s}}}(n_j,f)\right]\mathbf{U}^{T} + \frac{1}{T}\sum_{j=1}^{T}\mathbf{W}\bar{\boldsymbol{\omega}}(n)\bar{\boldsymbol{\omega}}^{T}(n)\mathbf{W}^{T} \quad (24)$$

Assuming noise $\bar{\boldsymbol{\omega}}(n)$ Gaussian, white and zero-mean the noise influence in (24) can be expressed as:

$$\lim_{T\to\infty}\frac{1}{T}\sum_{n=1}^{T}\mathbf{W}\bar{\boldsymbol{\omega}}(n)\bar{\boldsymbol{\omega}}^{T}(n)\mathbf{W}^{T}=\sigma^{2}\mathbf{W}\mathbf{W}^{T} \quad (25)$$

The noise variance σ^2 can be estimated from the correlation matrix $\mathbf{R}_{\bar{\mathbf{x}}}$, while the whitening matrix **W** is known. This allows us to simply subtract the noise influence in (24).

The influence of noise can further be reduced by averaging the reconstructed sources $\bar{\mathbf{s}}(n)$. Namely, presented decomposition approach reconstructs *(L+K-1)* delayed repetitions of each source, which can be aligned in time and averaged afterwards.

4 SEMG decomposition results

The presented decomposition approach was tested on synthetic and real SEMG signals. As already explained in the Section 2, the MU can be treated as a pulse sources, while the innervation trains of different MUs do not overlap significantly (at least at low muscle contraction levels). On the other hand, the assumption of the stationary mixing matrix imposes the surface EMG measurements must be taken in steady, controlled isometric conditions.

4.1 Results on synthetic SEMG signals

The proposed decomposition procedure was first tested on synthetic SEMG signals, generated using the advanced surface EMG simulator [8]. The volume conductor was described as an anisotropic layered medium with muscle, fat and skin layers. Active MUs consisted of a random number of fibers (uniformly distributed between 50 and 300) with the circular MU territories of 20 fibres/mm^2. Detection system with 11 rows and 5 columns of electrodes was centred over the distal half of muscle fibers, simulating 50 single-differential measurements of surface EMG. The number of active MUs was set to 5 and 10, respectively, while SNR ranged from 10 dB to 20 dB, in steps of 5 dB. 10 simulations were

performed for each number of active MUs. In each of the simulation runs the depth of the active MUs, their discharge rate, number of fibers, shift in the direction transversal to the muscle fibers, and conduction velocity were randomly selected. Signals from each simulation run were corrupted by additive noise (5 realizations of noise for each SNR).

The described decomposition method assumes the number of sources is known. Note however, the number of sources can be overestimated. As a result, the method reconstructs some extra sources, but they all have amplitude close to zero. Nevertheless, testing the method on the synthetic signals, we supposed the number of sources was known. The vector of measurements was extended by factor K=3 in the case of 5 active MUs, and by factor K =7 in the case of 10 active MUs, resulting in 135 and 310 extended sources, respectively. The measurements were first whitened and STFD matrices were calculated. Afterwards, the criterion (23) was used to select candidates for joint diagonalization (in order to reduce the influence of noise, up to 20 different STFD matrices were summed together, as described in (24)). Finally, the reconstructed repetitions of the same source were aligned in time and averaged. The results are summarized in Table 1 and Figs. 1 and 2.

4.2 Results on real SEMG signals

The real experiments were conducted with signals from the dominant biceps brachii of nine healthy male subjects (age 26.8 ± 2.2 years, height 179 ± 7 cm and weight of 72.1 ± 8.3 kg). All subjects gave their informed consent. The signals were detected by an array of 13×5 electrodes (size of 1×1 mm and inter-electrode distance of 5 mm), amplified (gain set to 10000) by a 64-channel EMG amplifier (LISiN; Prima Biomedical & Sport, Treviso, Italy), band-pass filtered (-3 dB bandwidth, 10 Hz – 500 Hz), and sampled at 2500 Hz by 12-bit A/D converter. The signals were recorded during the 30 s long isometric voluntary muscle contractions sustained at constant level of 5% and 10% of maximum voluntary contraction (MVC), respectively. The contraction force was measured by the torque sensor and displayed on the oscilloscope to provide the visual feedback to the subjects. The noise and movement artefacts were visually controlled and reduced by applying water to the skin surface.

Following the protocol in the first experiment, we first supposed the number of active MUs limited to 7 in the case of 5% MVC, and to 10 in the case of 10% MVC. Consequently, the measurements were extended by the factor K=10 at 5 % MVC, and K=15 at 10 % MVC. The results of the decomposition are summarized in Table 2 and Figs. 3 and 4.

Table 1. The number of reconstructed MU (mean ± standard deviation), the percentage of accurately reconstructed pulses (true positive statistics) and the percentage of misplaced pulses (false positive statistics).

No. of MUs	SNR [*dB*]	No. of reconst. MU	True Positive [%]	False Positive [%]
5	20	3.8 ± 0.9	90.0 ± 12.0	5.9 ± 6.0
	15	3.3 ± 1.3	81.6 ± 14.6	7.5 ± 7.0
	10	2.8 ± 0.9	77.3 ± 16.0	12.7 ± 8.7
10	20	7.3 ± 1.1	89.0 ± 14.7	5.0 ± 8.7
	15	6.1 ± 0.8	83.9 ± 14.2	5.9 ± 8.9
	10	4.7 ± 1.0	76.7 ± 14.5	9.4 ± 11.0

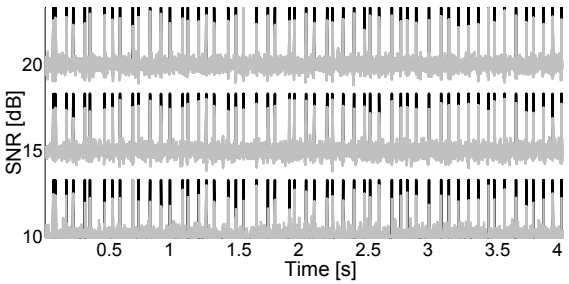

Fig. 1: Original synthetic innervation pulse trains (black) and reconstructed pulse trains (grey) in the case of 5 active MUs.

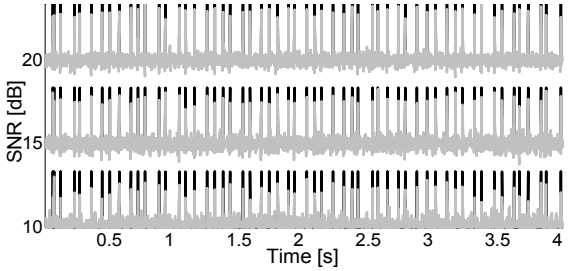

Fig. 2: Original synthetic innervation pulse trains (black) and reconstructed pulse trains (grey) in the case of 10 active MUs.

4 Conclusion

The results in Table 1 show the efficiency of presented decomposition approach decreases with the SNR and the number of active MUs. At SNR of 20 dB, the average number of the reconstructed MUs yields 3.8 and 7.3 in the case of 5 and 10 MUs, respectively. Decreasing SNR to 10 dB the average number of MUs drops to 2.8 and 4.7.

The fact that the performance drops with the number of active MUs should not come as a surprise. At a high SNR, the criterion ensures that only the STFD matrices comprising the contribution from a single source enter the joint-diagonalization.

Low SNR and large number of active MUs, on the other hand, degrade the selection of STFD matrices and the negative impact of crossterms in STFD matrices increases.

Table 2. The number of reconstructed MUs and their average instantaneous firing rate. Surface SEMG signals were recorded during the isometric contractions of the dominant biceps brachii of nine healthy male subjects.

MVC [%]	Number of reconstructed MU	Average firing rate (pulses per second)
5	2.6 ± 0.7	13.2 ± 1.4
10	3.0 ± 1.0	14.0 ± 1.9

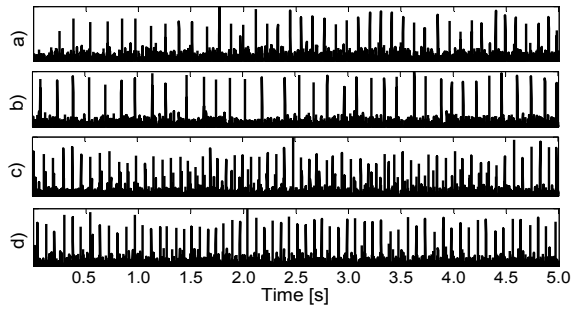

Fig. 3: Reconstructed MU innervation pulse trains in the case of 5 % MVC contraction of biceps brachii: a) subject 1, MU 1 b) subject 1, MU 2, c) subject 2, MU 1, d) subject 2, MU 2.

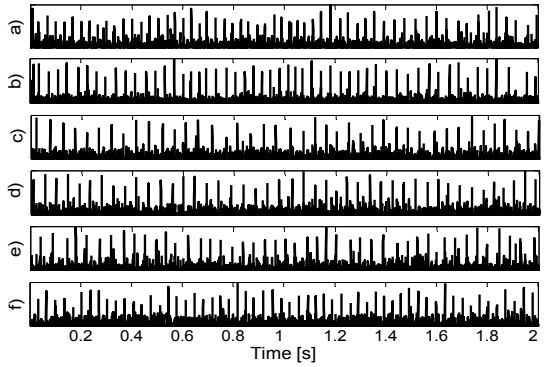

Fig. 4: Reconstructed MU innervation pulse trains in the case of 10 % MVC contraction of biceps brachii: a) subject 1, MU 3 b) subject 6, MU 1, c) subject 6, MU 3, d) subject 6, MU 4, f) subject 8, MU 3.

Evaluating the results on the real surface EMG the original MU firing patterns and the reference MUAP shapes are unknown. However, encouraged by the results on the synthetic signals, we can rely on less strict measures, such as calculated instantaneous discharge rate and regularity of reconstructed inter-pulse intervals. Finally, MUAPs as detected by the electrodes can be extracted by spike triggered averaging (using the identified discharge instants as triggers) and taken into account. In the case of 5 % MVC real measurements a total of 23 MUs were identified. When decomposing the 10 % MVC measurements, the total number of identified MUs reached 27. In both cases the average MU firing rate was within expected physiological limits (from 8 to 15 pulses per second). The extracted MUAPs exhibited stable shape over time revealing location of MU innervation zones, length of the fibers, and propagation in the fiber direction.

The proposed TF-based method can extract MU discharge patterns in low-level isometric conditions, is not sensitive to MUAP superimpositions and has potential clinical applications for the non-invasive analysis of single MU properties.

References:

[1] A. Belouchrani, K. Abed-Meraim, J.-F. Cardoso, E. Moulines, A blind source separation technique using second-order statistics, *IEEE Trans. Sig. Proc.*, Vol. 45, No. 2, 1997, pp. 434-444.

[2] A. Belouchrani, M.G. Amin, Blind source separation based on time-frequency signal representations, *IEEE Trans. Sig. Proc.*, Vol. 46, No. 11, 1998, pp. 2888-2897.

[3] B. Boashash, *Time-frequency signal analysis and processing*, Prentice Hall PTR, Englewood Cliffs, New Jersey, 2001.

[4] J. F. Cardoso, A least-squares approach to joint diagonalization, *IEEE Sig. Proc. Lett.*, Vol. 4, 1997, pp. 52-53.

[5] J. F. Cardoso, Perturbation of joint diagonalizers. *Technical report ref.# 94d027*, Télécom Paris, 1994.

[6] J. F. Cardoso, A. Souloumiac, Jacobi angles for simultaneous diagonalization, *SIAM Journal on Matrix Analysis and Applications*, Vol. 17, No. 1, 1996, pp. 161-164.

[7] L. Cohen, *Time-frequency analysis*, Prentice Hall PTR, Englewood Cliffs, New Jersey, 1995.

[8] D. Farina, R. Merletti, A novel approach for precise simulation of the EMG signals detected by surface electrodes, *IEEE trans. Biomed. Eng.*, Vol. 48, 2001, pp. 637-646.

[9] A. Holobar, C. Fevotte, C. Doncarli in D. Zazula, Single autoterm selection for blind source separation in time-frequency plane, *in Proc. EUSIPCO'02*, Toulouse, France, 2002, on CD.

[10] R. Merletti: Surface electromyography: possibilities and limitations, J. of Rehab. Sci., Vol. 7, No. 3, 1994, pp. 25-34.